Pergamon

Chemical Engineering Science, Vol. 51, No. 9, pp. 1509–1521, 1996

0009–2509/96 $15.00 + 0.00

0009–2509(95)00306–1

ON PHYSIOLOGICAL MULTIPLICITY AND POPULATION HETEROGENEITY OF BIOLOGICAL SYSTEMS

JOHN D. CHUNG and GREGORY STEPHANOPOULOS*
Department of Chemical Engineering, Massachusetts Institute of Technology, Cambridge, MA 02139, U.S.A.

(*First received* 31 *May* 1994; *revised manuscript received and accepted* 13 *February* 1995)

Abstract—The theory of steady-state multiplicity has been used to analyze the adaptive behavior associated with two experimentally well characterized biological systems; the bacteriophage λ and the *Escherichia coli* lactose operon. The ability to observe such systems in distinct physiological forms within a unique environment was found to be consistent with the existence of multiple stable solutions of the representative balance equations. Additionally, transitions between physiological states were found to be controlled by threshold mechanisms that altered the steady-state solution structure in a manner analogous to the ignition-extinction behavior exhibited by non-isothermal chemical reactors. These findings indicate that the population heterogeneity observed in these systems can be explained on the basis of steady-state multiplicity whereby a nonuniform population response acts to generate a culture comprised of physiologically distinct forms. Since multiple solutions of the conservation equations were found to originate from interactions between conserved nonlinear kinetic and feedback mechanisms, these results appear general and the conclusions derived should be applicable to other less characterized biological systems. These findings also suggest that the physiological homogeneity assumption routinely employed in theoretical and experimental analysis of cellular behavior may lack theoretical justification.

1. INTRODUCTION

There are many biological systems that have been observed to exist in different physiological forms under identical environmental conditions. A simple example is provided by the bacteriophage λ which, under the appropriate conditions, can exist in one of two forms (Bailone *et al.*, 1979). A more complex example arises with differenting cultures of *Bacillus subtilis* where heterogeneity among transcriptional states has been observed early during development (Chung, 1994; Chung *et al.*, 1994), Even in systems that do not undergo development there can exist physiological heterogeneity. Under certain conditions, it is possible to generate a heterogeneous culture of cells of *Escherichia coli* where one population is induced for expression of the lactose operon and the other remains uninduced (Benzer, 1953; Novick and Weiner, 1957; Maloney and Rotman, 1973). Such physiological variations are often attributed to different accumulation of important cellular components (Novick and Weiner, 1957; Horvitz and Herskovitz, 1992; Chung *et al.*, 1994). At a 'threshold' concentration, a 'switch' is thrown and this somehow leads to the generation of an alternate biological form. Unfortunately, proving this premise is difficult since it requires the monitoring of the intracellular concentration of such components within individual cells. Even with the best characterized genetic system the *E. coli* lactose operon, experimental support for the 'threshold' hypothesis is indirect and theoretical explanations are incomplete or tenuous (Novick and Weiner, 1959; Maloney and Rotman, 1973).

The purpose of this paper is twofold. Due to the influential role that the threshold hypothesis has in shaping our view of biological systems, the first objective of this paper is to provide a more precise undertaking of this hypothesis and its implications through the use of theoretical arguments. Theoretical studies on two well-characterized genetic systems, the lysis-lysogeny response of bacteriophage λ and the induction of the *E. coli* lactose operon, are initiated with the purpose of understanding how distinct biological forms might be generated and how they can coexist in the same environment. The lysis-lysogeny response involves λ's decision to remain dormant within the host cell, as a lysogen, or to initiate lytic development whereby it rapidly reproduces and subsequently destroys its host [see Ptahsne (1987) for review]. The induction of the lactose operon involves the cell's decision whether or not to express those genes under the operon's control. The results of these studies will also make it possible to understand how critical concentrations of intracellular components can initiate behavioral switches as well as provide estimates of the concentrations responsible.

Looking beyond the specifics of the two systems considered, the second objective of this paper is to demonstrate that principles developed in chemical reaction engineering provide a useful structure in which to analyze basic biological data, obtained from seemingly unrelated phenomena, so as to provide further insights into the behavior of such systems under a variety of conditions. The ignition-extinction

* Corresponding author.

techniques used in the analysis of multiple chemical reactor operating states are used to identify multiplicities in cellular physiological states and to reveal the biochemical causes of such multiplicities. Within this framework, physiological heterogeneity is associated with the existence of multiple stable solutions of the governing conservation equations, and adaptation concerns itself with transitions between these states. Often times, molecular biological research is criticized for the lack of measurements (Maddox, 1992). However, even in those cases where measurements are reported, a quantitative framework of this nature would be of value to determine whether (a) the parameters measured are sufficient or even the right ones and, (b) how they can best serve to elucidate the understanding of the biological systems at hand.

The principal conclusions derived from this work are that threshold mechanisms regulate the adaptive responses associated with both systems analyzed and that the existence of such mechanisms provides the potential for generating physiological diversity. Interactions between nonlinear kinetic and feedback mechanisms were found to give rise to the existence of threshold mechanisms. Since thresholds inherently initiate all-or-none cellular responses, suboptimal culture responses apparently reflect averages taken over a heterogeneous population and not events occurring at the cellular level. With the lactose operon, suboptimal induction conditions lead to the generation and maintenance of a heterogeneous culture comprised of fully induced and uninduced cell types. With bacteriophage λ, suboptimal induction conditions initiate fewer lysogens into the pathway of lytic development. Given the relative simplicity of the systems analyzed and the major role that these systems have played in establishing our understanding of gene expression and regulation, we argue that the conclusions obtained are general and that thresholds can be expected to exist in all biological systems that contain similar regulatory mechanisms.

2. BACTERIOPHAGE λ

2.1. *Background*

We begin with an analysis of the phage λ, a genetic system that has played an important role in establishing our present understanding of development. Under the appropriate conditions, lysogens of *E. coli* may opt to initiate lytic development (Jacob and Monod, 1961; Bailone *et al.*, 1979; Ptashne, 1987). Once induced, a developmental program of gene expression is initiated which culminates in the maturation of phage particles and the subsequent lysis of the host.

At the molecular level the lysis-lysogeny switch is controlled by the intracellular concentration of CI, the *cI* gene product [see Ptashne (1987) for review]. CI, often referred to as λ repressor, is present in lysogens and it plays a critical role in maintaining lysogeny. This is achieved by promoting its own synthesis so as to provide a sufficient level of CI to prevent lytic development by repressing the lytic specific gene *cro*. Only after the concentration of CI falls below a critical level, is repression relieved and lytic development initiated.

These findings suggest that a more precise understanding of this phenomenon can be obtained through a quantitative description of how phage regulates the intracellular concentration of λ repressor. In the following sections, cellular material balances are used to achieve this goal.

2.2. *A rate equation for CI generation*

An expression for the rate of repressor generation is now derived assuming that the generation of repressor is limited at the level of transcription. This assumption is reasonable as adaptive cellular processes are often regulated at the level of transcription.

During lysogeny, transcription from *cI* is regulated by the binding of CI dimer to three adjacent binding sites, O_R1, O_R2 and O_R3, that comprise what has been termed the O_R operator [Fig. 1, Johnson *et al.* (1981) and Ptashne (1987)]. Together these sites overlap regions of both the *cI* and *cro* promoters, P_{RM} and P_R, respectively. Because the relative binding affinities of dimer for these sites is such that O_R1 is first filled followed by O_R2 then O_R3, *cro* will be repressed so long as CI is present in sufficient quantities within the cell since the O_R1 site lies within the *cro* promoter sequence P_R. In contrast, once CI dimer binds to O_R2, it facilitates the ability of RNA polymerase to recognize P_{RM}, via protein–protein interactions, and transcription of *cI* is stimulated approximately tenfold (Ptashne, 1987). However, as CI accumulates, O_R3 is filled and transcription of *cI* is repressed since the O_R3 binding site lies within the *cI* promoter P_{RM}. While other bound configurations of O_R exist (Ackers *et al.*, 1992), thermodynamic computations indicate that the described scenario accounts for greater than 92% of the possible configurations. Therefore for simplicity, it is assumed that CI dimer binds to O_R only in the order described. Additionally, it will also be assumed that transcription of *cI* is initiated only after *both* O_R1 and O_R2 are occupied since transcription from other operator configurations is negligible (Ptashne, 1987). Under these assumptions, the rate of generation of CI is given by

$$R_{GEN} = k_1[O(CI)_2(CI)_2]. \tag{1}$$

Equation (1) states that the rate of generation of CI is proportional to the concentration of the doubly occupied operator, $[O(CI)_2(CI)_2]$, where (CI_2) denotes the dimeric form of λ repressor. The proportionality or the first-order rate constant is given by k_1. An equivalent interpretation of this equation is that the generation rate is proportional to the probability that O_R will exist as $O(CI)_2(CI)_2$.

A useful expression is obtained by replacing $[O(CI)_2(CI)_2]$ with terms that have been determined experimentally. This is accomplished by assuming that the concentrations of the O_R sites and CI dimer

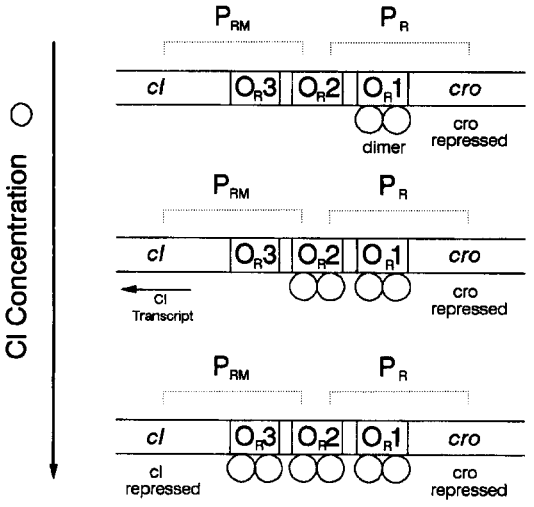

Fig. 1. Mechanism by which CI maintains lysogeny. At low [CI], CI activates its own transcription through the binding of dimer to the O_R2 and O_R3 sites of the O_R operator. At high [CI], transcription from *cI* is repressed. All configurations shown repress *cro* [adopted from Ptashne (1987)].

lie close to equilibrium. The reactions and their corresponding equilibria relationship are given by

$$[O] + [(CI)_2] = [O(CI)_2] \quad (2)$$

$$[O(CI)_2] + [(CI)_2] = [O(CI)_2(CI)_2] \quad (3)$$

$$[O(CI)_2(CI)_2] + [(CI)_2] = [O(CI)_2(CI)_2(CI)_2]. \quad (4)$$

with

$$K_1 = \frac{[O(CI)_2]}{[O][(CI)_2]} \quad (5)$$

$$K_2 = \frac{[O(CI)_2(CI)_2]}{[O(CI)_2][(CI_2)]} \quad (6)$$

$$K_3 = \frac{[O(CI)_2(CI)_2(CI)_2]}{[O(CI)_2(CI)_2][(CI_2)]} \quad (7)$$

where [O], $[O(CI)_2]$ and $[O(CI)_2(CI)_2(CI)_2]$ denote the concentrations of the free, singly and triply occupied operator, respectively. The final relationship needed, the O_R conservation equation, is given by

$$[O_T] = [O] + [O(CI)_2] + [O(CI)_2(CI)_2] + [O(CI)_2(CI)_2(CI)_2] \quad (8)$$

where $[O_T]$ denotes the total operator concentration. Solving eqs (2)–(8) for $[O(CI)_2(CI)_2]$ and substituting the result into eq. (1) yields

$$R_{GEN} = \frac{k_1 K_1 K_2 [O_T][(CI)_2]^2}{1 + K_1[(CI)_2] + K_1K_2[(CI)_2]^2 + K_1K_2K_3[(CI)_2]^3}. \quad (9)$$

Equation (9) relates the rate of CI generation to $[(CI)_2]$, equilibrium parameters, k_1 and $[O_T]$. Except for the kinetic parameter k_1, the value of all parameters can be found in the literature (Table 1).

Table 1. Parameters used in phage λ model

Parameter	Value*	Source†
$[O_T]$	1×10^{-9} M	Johnson *et al.* (1981)
K_A	5×10^{7} M^{-1}	Ackers *et al.* (1982)
K_1	1.77×10^{8} M^{-1}	Ackers *et al.* (1982)
K_2	3.40×10^{8} M^{-1}	Ackers *et al.* (1982)
K_3	1.32×10^{8} M^{-1}	Ackers *et al.* (1982)
k_2, k_3	0.023 min^{-1}	$k_i = \ln 2/\tau_d$

*The K_i's were calculated using $\Delta G_i = -RT \ln K_i$ evaluated at 37°C. K_2 includes the cooperative free energy resulting from $O_R1 - O_R2$ interactions.
†τ_d represents the cell-doubling time.

2.3. *Single cell material balances*

Single cell molar balances on [CI] and $[(CI)_2]$ are now derived in order to demonstrate how R_{GEN} determines the fate of phage. Assuming the cell is a well mixed variable volume chemical reactor and repressor cannot cross its boundaries, general cellular molar balances on [CI] and $[(CI)_2]$ are given by

$$\frac{d([CI]V_c)}{dt} = (\Sigma R_{GEN_i} - \Sigma R_{DEGR_j})V_c \quad (10)$$

$$\frac{d([(CI)_2]V_c)}{dt} = (\Sigma R_{GEN_k} - \Sigma R_{DEGR_l})V_c. \quad (11)$$

The R_{GEN}'s and R_{DEGR}'s represent the molar rates of repressor generation and removal, respectively, with V_c denoting the cell volume. Contributions to the summation terms are assumed to be limited to R_{GEN} and the forward and reverse reactions associated with the dimerization reaction:

$$2[CI] = [(CI)_2]. \quad (12)$$

The equilibrium constant associated with this reaction is written in terms of the forward and reverse reaction rates as

$$K_a = \frac{k_f}{k_r} = \frac{[(CI)_2]}{(CI)^2}. \quad (13)$$

Substituting the contributions from the dimerization reaction into eqs (10) and (11) yields

$$\frac{d([CI])}{dt} = R_{GEN} + k_r[(CI)_2] - k_f[CI]^2 - k_2[CI] \quad (14)$$

$$\frac{d([CI]_2)}{dt} = -\frac{k_r}{2}[(CI)_2] + \frac{k_f}{2}[CI]^2 - k_3[(CI)]_2 \quad (15)$$

where the forward and reverse rate constants, k_f and k_r, *are based on moles of monomer*. The last term, on the right-hand side of both equations, represents the dilution effect due to cell growth.

In deriving eqs (14) and (15), mechanisms that account for the specific degradation of [CI] and $[(CI)_2]$ have been ignored. When such processes cannot be

ignored, first-order kinetic mechanisms can be assumed and the base values of k_2 and k_3, given by

$$k_2 = k_3 = \frac{1}{V_c}\frac{dV_c}{dt} \tag{16}$$

are altered accordingly.

2.4. *The steady-state solutions*

Combining the steady-state forms of eqs (14) and (15) with eq. (9) yields

$$[(CI)_2] = K_A[CI]^2 \tag{17}$$

$$2k_2K_A[CI]^2 + k_2[CI] = \frac{k_1K_1K_2[O_T]K_A^2[CI]^4}{1+K_1K_A[CI]^2+K_1K_2K_A^2[CI]^4+K_1K_2K_A^3[CI]^6} \tag{18}$$

with

$$K_A = K_a\frac{1}{1+\dfrac{2k_3}{k_r}}. \tag{19}$$

The simplest interpretation of eq. (18) is that, for the cell to maintain homeostasis during balanced growth, the rate of repressor generation must be balanced by the rate of repressor removal. The right-hand side of eq. (18) is simply the rate of CI generation, eq. (9), in terms of [CI]. The left-hand side of eq. (18) represents the rate of repressor removal due to growth with the quadratic term representing the dilution of $[(CI)_2]$.

These equations determine the intracellular concentrations of [CI] and $[(CI)_2]$ under balanced growth conditions. This is graphically illustrated in Fig. 2 where a repressor removal rate curve is superimposed on a series of repressor generation curves. These curves were calculated using the values in Table 1 with k_1 as parameter. Since the points of intersection between these curves identify real solutions of eq. (18), three real solutions exist in the parameter range defined by Table 1.

Stable solutions of eq. (18) represent the physiological states available to phage. The lysogenic state corresponds to the stable steady state at large [CI]. At these concentrations, phage stably maintains lysogeny by adjusting the rate of repressor generation to meet the demands placed on it by cell growth. Since lytic development is characterized by little or no expression of CI, the intersection at the origin may be interpreted as representing this process. Separating these physically observable states is an unstable state which acts as a physiological boundary. [CI] values above this boundary are sufficient to maintain lysogeny. In contrast, repressor concentrations below this boundary direct phage to lytic development.

The theoretical framework developed allows kinetic information to be determined from concentration data reported in the literature. This is illustrated in Fig. 2 where dashed vertical lines are used to identify the lower and upper repressor concentration boundaries reported in the literature. These values correspond to *total* repressor concentrations of 1×10^{-7} and 2×10^{-7} M, respectively, or 100 or 200 molecules of repressor per cell assuming a cell volume of 1×10^{-15} (Pirrotta *et al.*, 1970; Ackers *et al.*, 1982). The solutions of eq. (18) found within this concentration region indicate that the rate constant k_1 is

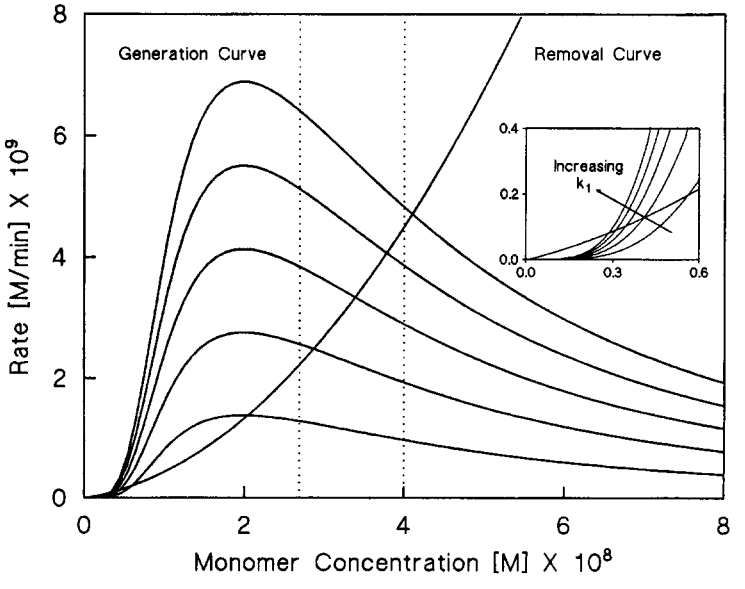

Fig. 2. Graphical determination of the real positive solutions of eq. (17) as represented by the intersections between the removal and generation curves. The generation curves shown are for $k_1 = 2$, 4, 6, 8 and 10 min^{-1}. The removal curve has been set by the cell doubling time. One solution exists at high CI and two at low CI (inset). Repressor concentration data reported in the literature (i.e. the region between the dotted lines) may then be used to determine a range of k_1's.

between 4 and 8 min^{-1}. In subsequent sections, a k_1 of 4 min^{-1} is shown to lead to behavior that is consistent with a number of experimental observations.

2.5. *Inducing lytic development*

The effects of lysis inducing agents may be mathematically represented by an increased value of k_2. In the laboratory, lytic development is induced by stimuli that activate the proteolytic activity of RecA (Bailone *et al.*, 1979; Ptashne, 1987). RecA is a protein that is normally involved in catalyzing recombination between DNA molecules (Ptashne, 1987). However, when DNA is damaged, RecA acts as a protease and degrades the monomeric form of λ repressor. According to eq. (14), the specific degradation of [CI] may be accounted for by altering the value of k_2.

The constant k_2 can be viewed as a threshold or bifurcation parameter. Figure 3 illustrates how the number of solutions of eq. (18) is altered as k_2 is increased. Since small increases in k_2 preserve the number of solutions, the lysogenic state is stable with respect to small physiological perturbations. However, as the severity of the perturbation is increased, the capacity of phage to maintain lysogeny is exceeded. When this occurs, at a value of k_2 around seven times the growth rate, the stable solution at large [CI] no longer exists. Under these conditions, a rate imbalance is created such that the only state available to phage is associated with lytic development. Since k_2 principally reflects the action of RecA, these results indicate that activated RecA must reach a threshold concentration before lytic development can be initiated. Considering that, in general, RecA activation reflects the action of an external inducing agent, this conclusion is consistent which the observation that the degree of induction can be altered by varying the dosage of UV radiation (Bailone *et al.*, 1979).

2.6. *Commitment to lytic development*

The repressor concentration at the intermediate unstable steady state determines, in part, the point of commitment. The dynamics associated with the initial stages of induction are described in Fig. 4 where time course profiles of [CI], resulting from transient perturbations in the value of k_2, have been determined via eqs (14) and (15). The perturbed value of k_2 was chosen to be slightly greater than the threshold value (Fig. 3) to reflect the fact that all lysogens do not complete development. Transient perturbations were used to simulate the transient action of RecA proteolysis (Bailone *et al.*, 1979). Following a 30 min perturbation, phage is able to reestablish lysogeny despite a decrease in intracellular repressor. In contrast, a one minute further increase in the duration of the perturbation is sufficient to commit phage to lytic development. Commitment results because [CI] has been driven to just below the concentration at the intermediate unstable steady state. Therefore, after the perturbation is removed and the original eq. (16) solution profile is reestablished, the new [CI] places phage on the lytic side of the physiological boundary.

These results are consistent with a number of experimental findings. Bailone and coworkers (1979) found that fewer lysogens completed lytic development when transiently subjected to thymine

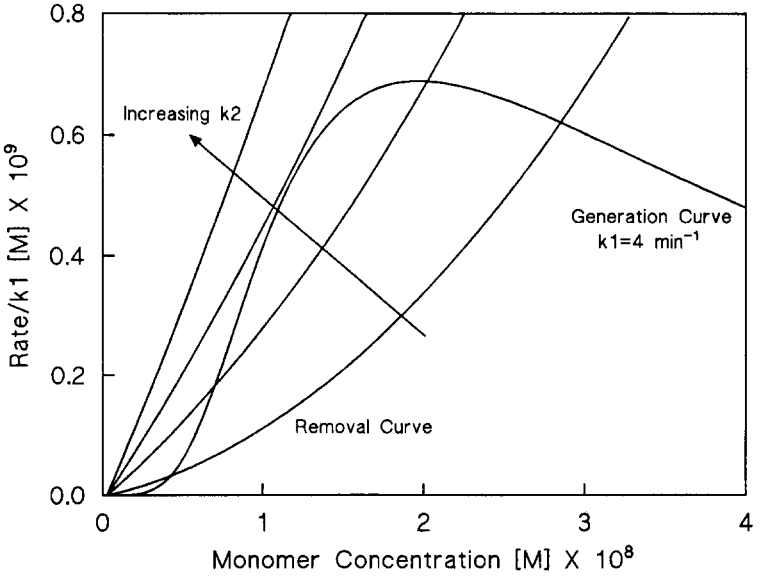

Fig. 3. Initiating lytic development via a threshold mechanism. As k_2 is slowly increased, a point is reached where the system can no longer adjust to the increased 'stress'. This results in the abandonment of lysogeny and the subsequent induction into lytic development. The removal curves were constructed for k_2 = 0.023, 0.092, 0.162 and 0.254 min^{-1}.

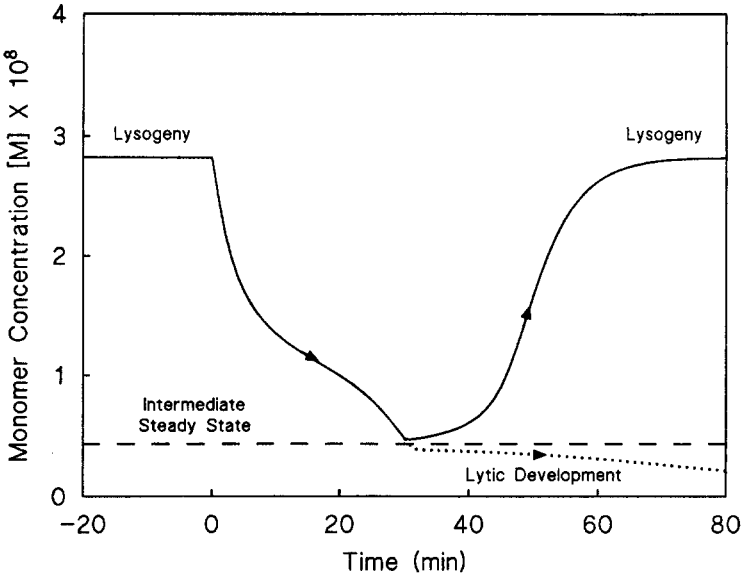

Fig. 4. Transient responses of [CI] following 30 and 31 min square-wave perturbations in k_2 at time 0 (0.023 to 0.184 to 0.023 min^{-1}). In generating these profiles, it was assumed that $[(CI)_2]$ rapidly equilibrates with [CI] or equivalently that changes in [CI] during RecA proteolysis are slow relative to the dissociation of $[(CI)_2]$. Since the dissociation of dimer is rapid (Chadwick *et al.*, 1970), this assumption is reasonable.

starvation. Additionally, the value of [CI] at the unstable steady state indicates that approximately 95% of the repressor present in lysogens must be degraded in order to commit phage to lytic development. This estimate is in good agreement with the experimentally determined value of 90% reported by Bailone and coworkers (1979). Finally, for the k_2 value chosen, the time duration until phage is committed is of the order of 30 min. A similar time constant was determined experimentally by Bailone and coworkers (1979).

3. THE *E. coli* LACTOSE OPERON

3.1. *Background*

The second system analyzed, the *E. coli* lactose operon, principally differs from phage in that it does not involve terminally differentiating entities (Benzer, 1953; Novick and Weinger, 1957, 1959; Cohn and Horibata, 1959; Maloney and Rotman, 1973). Therefore, in addition to studying the origins of physiological heterogeneity, this system provides the means of studying reversibilities associated with adaptation. Furthermore, because the state acquired by the operon has been found to depend on the cell's previous history (Novick and Weiner, 1957), this analysis will help to identify some of the basic components of cell memory.

At the molecular level, induction of the operon in a nonglucose containing medium by a nonmetabolizable inducer is controlled by a positive feedback loop involving *lac* permease, *lac* repressor and *lac* inducer (Fig. 5). In the absence of inducer, transcription of the operon is repressed by the binding of repressor to the *lac* operator. However, when inducer is added to the culture medium, it enters the cell where it may indirectly initiate transcription by binding to the repressor so as to reduce repressor's affinity for the operator. Once the repressor is disengaged from the operator, transcription may be initiated. Since *lac* permease, a gene product of the operon, serves to import inducer, it positively affects its own expression.

3.2. *A rate equation for permease generation*

Since *lac* permease plays an important role in the induction process, we begin by deriving an expression to describe its rate of generation. Assuming that the permease generation rate is limited at the level of transcription, the rate of permease generation may be represented by

$$R_{GEN} = k_1[O] \tag{20}$$

where [O] denotes the concentration of free *lac* operator and k_1 denotes the first-order kinetic constant which is conceptually similar to the k_1 used in the phage study

The reaction leading to the inactivation of repressor is represented by

$$2[I] + [R] = [I_2R] \tag{21}$$

where [I], [R], and $[I_2R]$ denote the concentrations of free inducer, free repressor and inducer-repressor complex, respectively. The binding of free repressor to the operator is represented by

$$[R] + [O] = [RO] \tag{22}$$

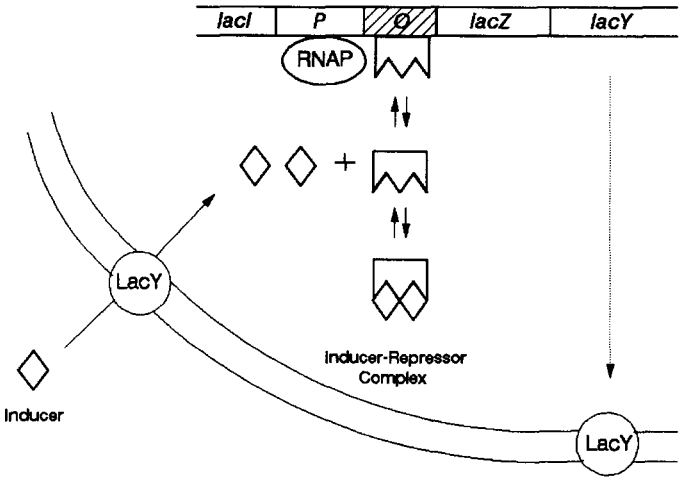

Fig. 5. Schematic of the autocatalytic mechanism used by cells to regulate the state of the lactose operon. When inducer is present in the extracellular medium, it may enter the cell and bind to repressor. Since the inducer–repressor complex has a low affinity for the operator, the probability of finding the operator free of repressor increases as does the chance that the operon will be transcribed. Positive feedback results from permease's (i.e. the *lacY* gene product) ability to concentrate intracellular inducer.

where [RO] denotes the concentration of the repressor–operator complex. The associated equilibrium constants are defined by

$$K_1 = \frac{[I_2R]}{[R][I]^2} \tag{23}$$

$$K_2 = \frac{[RO]}{[R][I].} \tag{24}$$

Site balances on total operator and total repressor are given by

$$[O_T] = [O] + [RO] \tag{25}$$

$$[R_T] = [R] + [I_2R] \tag{26}$$

where $[R_T]$ and $[O_T]$ denote the total concentrations, bound and unbound, of repressor and operator, respectively. Equation (26) neglects [RO] relative to [R] since the concentration of repressor is typically much greater than the concentration of operator. After algebraic manipulations, the rate of permease generation is given by

$$R_{GEN} = k_1[O_T]\frac{1 + K_1[I]^2}{1 + K_1[I]^2 + K_2[R_T]}. \tag{27}$$

Equations (21) and (27) incorporate an important detail that is often omitted in other treatments of the same system (Bailey and Ollis, 1986; Darnell *et al.*, 1990; Laffend and Shuler, 1994). Namely, that the inactivation of *lac* repressor and the eventual induction of the operon, requires that *two* inducer molecules bind to the repressor complex (Boezi and Cowie, 1961; Yagil and Yagil, 1971; Barkley and Bourgeois, 1980) as opposed to one molecule which is most often assumed. This detail yields the nonlinear $[I]^2$ term in the numerator of eq. (27). When the operon is fully induced, this nonlinearity is of little consequence since the generation rate is saturated with respect to increasing [I]. However, failure to account for this detail under suboptimal induction conditions leads to a dramatically different dynamic system.

3.3. *Single cell material balances*

Molar balances on cell-associated *lac* permease and *lac* inducer are given by

$$\frac{d([Y]V_c)}{dt} = R_{GEN}V_c \tag{28}$$

$$\frac{d([I]V_c)}{dt} = (R_{ACTIVE} + R_{FACILITATED})V_c \tag{29}$$

where [Y] and [I] denote the cell-associated permease and inducer concentrations, respectively, and R_{GEN} represents the permease generation rate. R_{ACTIVE} represents the rate of active transport of inducer via permease and $R_{FACILITATED}$ represents the rate of transport of inducer via *lac* permease-independent processes.

The rate of active transport may be represented by (Rickenberg *et al.*, 1956; Cohen and Monod, 1957; Kepes, 1960):

$$R_{ACTIVE} = \frac{\alpha[I_{EX}][Y]}{\beta + [I_{EX}]} \tag{30}$$

where α, β and $[I_{EX}]$ denote the permease turnover number, the permease saturation constant and the extracellular concentration of inducer, respectively. The turnover number represents the maximum number of inducer molecules that can be transported into the cell per time per permease.

$R_{FACILITATED}$ may be represented by

$$R_{FACILITATED} = \delta([I_{EX}] - [I]) \tag{31}$$

where δ denotes the transport coefficient (Kepes, 1960; Cohen and Monod, 1957). This functionality allows the concentration-dependent nature of facilitated transport to be represented (Herzenberg, 1959) and naturally leads to an equilibration between [I] and $[I_{EX}]$ in *lac-Y*$^-$ strains under balanced growth conditions (Kepes, 1960; Yagil and Yagil, 1971).

Substituting eqs (30) and (31) into eqs (28) and (29) yields

$$\frac{d[Y]}{dt} = R_{GEN} - k_2[Y]. \tag{32}$$

$$\frac{d[I]}{dt} = \frac{\alpha[I_{EX}][Y]}{\beta + [I_{EX}]} + \delta([I_{EX}] - [I]) - k_2[I]. \tag{33}$$

As before, terms involving k_2 reflect the dilution of [Y] and [I] due to growth. Without loss of generality, degradative processes can be incorporated into these equations by altering the base value of k_2 as defined by eq. (16).

3.4. *The steady-state solutions*

After algebraic manipulations eqs (27), (32) and (33) yield at steady state

$$x_1[I] - x_2 = k_1 \frac{\alpha[O_T]}{(\delta + k_2)k_2} \frac{1 + K_1[I]^2}{1 + K_1[I]^2 + K_2[R_T]} \tag{34}$$

$$[Y] = \frac{(\beta + [I_{EX}])}{\alpha[I_{EX}]}[(\delta + k_2)[I] - \delta[I_{EX}]] \tag{35}$$

with

$$x_1 = \frac{\beta + [I_{EX}]}{[I_{EX}]} \tag{36}$$

$$x_2 = (\beta + [I_{EX}])\frac{\delta}{\delta + k_2}. \tag{37}$$

Equation (34) represents a steady-state rate balance and may be interpreted similar to eq. (18). The right-hand side of eq. (34) represents the permease generation rate eq. (27), which has been scaled by $\alpha/[\delta + k_2)k_2]$ for later convenience. The left-hand side of eq. (34) reflects the loss of permease due to growth with similar scaling.

The stable solutions of eq. (34) define the different transcriptional states. Figure 6 superimposes a single removal rate curve on generation rate curves constructed from eq. (34) and Table 2 for three different values of k_1. Curve (1) indicates that at small k_1 (i.e. generation rate) a unique intersection between these curves exists near the origin. This solution represents the uninduced state of the operon. At large k_1 (curve 3), multiple solutions of eq. (34) exist, and the solution at large [I] may be interpreted as representing the induced state. As with phage, the unstable solution that separates the two stable solutions of eq. (34) acts as a physiological boundary.

The theoretical framework developed allows the kinetic parameter k_1 to be estimated from data reported in the literature. Novick and Wiener (1957) reported that in a maltose containing media, an $[I_{EX}]$ of approximately 25 μM thiomethy-β-galactoside (TMG) maintains induced cells in the induced state without inducing uninduced cells. However, below this concentration induced cells are unable to maintain the induced state. These observations indicate that this value of $[I_{EX}]$ represents a critical concentration and that small variations from this value lead to a change in the number of states available to the cell. This information allows the value of k_1 to be determined by adjusting the generation curve, via variations in k_1, until it exhibits a point of tangency with

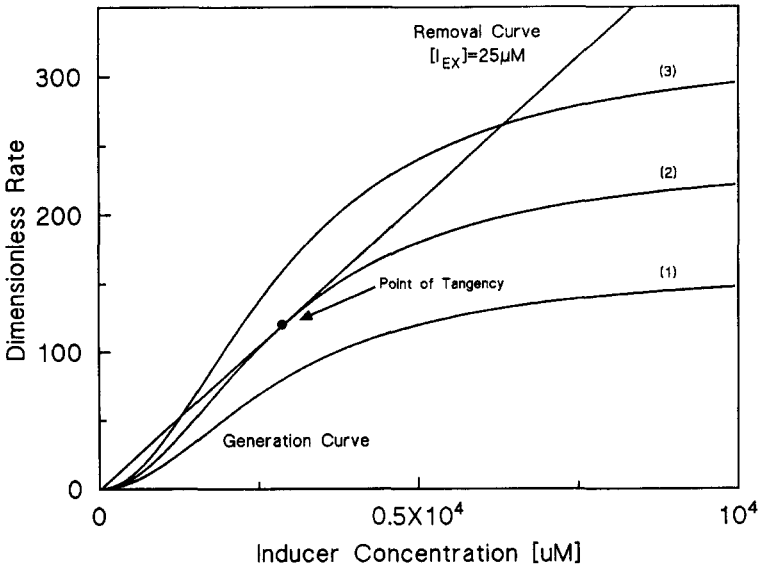

Fig. 6. Graphical determination of the solutions of eq. (34). The generation curves have been constructed using the parameters in Table 2 with $k_1 = 6$, 9 and 12 min^{-1}. Curve (2) allows the value of k_1 to be estimated using literature data.

Table 2. Parameters used in lactose operation model

Parameter	Value*	Source†
$[O_T]$	1×10^{-9} M	Johnson *et al.* (1981)
$[R_T]K_2$	1×10^5	Bourgeois and Monod (1970)
K_1	0.012 μM^{-2}	Barkley and Bourgeois (1980)
δ	0.82 min^{-1}	Kepes (1960)
β	500 μM	Kepes (1960)
k_2	0.0055 min^{-1}	$k_2 = \ln 2/\tau_d$
α	60,000 min^{-1}	Cohn and Horibata (1959)

*The value of K_1 listed is the square of the reported value since the reported value was determined based on the binding of one molecule of thiomethyl-β-D-galactoside (TMG) to repressor.

†τ_d represents the cell-doubling time.

the $[I_{EX}] = 25\ \mu M$ removal curve. This fit is illustrated in Fig. 6 (curve 2).

3.5. *Induction of gene expression*

The inducer concentration in the medium, $[I_{EX}]$, represents an experimental bifurcation or threshold parameter. Figure 7 illustrates how the number of real solutions of eq. (34) varies as $[I_{EX}]$ is increased. At low $[I_{EX}]$, the only state available to the cell is the uninduced state. This is represented by the unique solution near the origin. As $[I_{EX}]$ is further increased, the intersection at P2 is reached and any further increase in $[I_{EX}]$ results in three solutions of eq. (34) as reflected by the availability of the induced state. As discussed later, the stable nature of the uninduced state prevents the majority of the population from acquiring the induced state. As $[I_{EX}]$ is further increased, the removal curve eventually becomes tangent to P1 and any further increase results in the dissolution of the uninduced state. Extracellular inducer concentrations greater than that defined by P1 lead to the eventual induction of the population.

3.6. *Hysteresis and cell memory*

It has been observed that if the environment of an uninduced cell is altered by increasing the value of $[I_{EX}]$, then the cell acquires the induced state only at large $[I_{EX}]$ (Novick and Wiener, 1957). Intermediate $[I_{EX}]$ fail to induce uninduced cells. Similarly, if induced cells are placed in an environment containing intermediate $[I_{EX}]$, they remain induced. This apparent hysteresis in the transition from induced to uninduced states and vice versa, can be explained with the model developed as described below.

The totality of solutions of eq. (34) obtained by varying $[I_{EX}]$ over a range of values describes this phenomenon. This is illustrated by the curve shown in Fig. 8 which has been constructed by plotting all real positive solutions of eq. (34) against their corresponding $[I_{EX}]$. The branch of this curve beginning at small $[I_{EX}]$ and continuing to P1 identifies the locus of uninduced states. If the culture environment is altered by quasi-statically increasing $[I_{EX}]$, then the 'average' cell tracks this branch in the direction of the arrow until it reaches P1. Beyond P1, the capacity of the cell to maintain the uninduced state is exceeded and the cell experiences a "jump" as it seeks to acquire the induced state. The branch beginning at large $[I_{EX}]$ and continuing to P2 identifies the locus of induced states. Induced cells stay induced as long as $[I_{EX}]$ remains above the value defined by P2. The branch between P1 and P2 identifies the locus of experimentally unrealizable unstable solutions. The state of the operon depends on the cell's past history and this

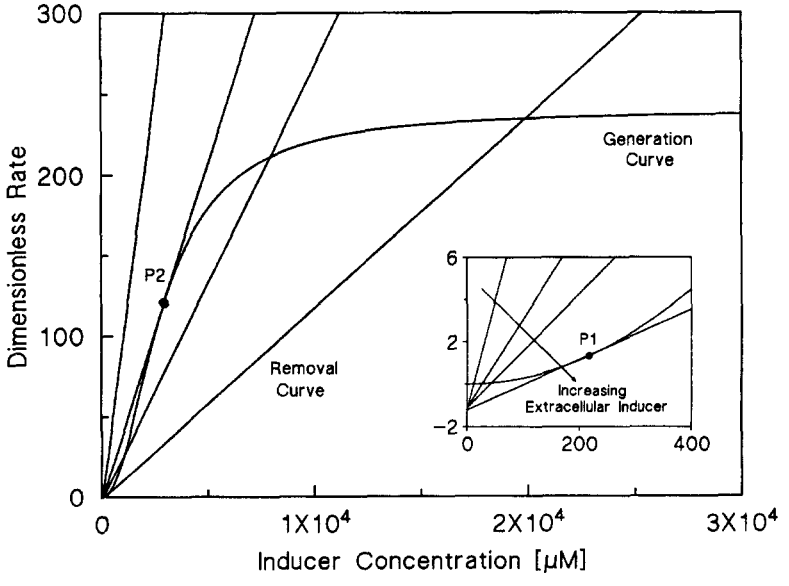

Fig. 7. Bifurcations in the number of solutions of eq. (34) as the experimental parameter $[I_{EX}]$ takes on the values of 10, 25, 40 and 100 μM TMG with $k_1 = 9\ min^{-1}$. For $[I_{EX}]$ on the order of 10 μM, only the uninduced state exists. For $[I_{EX}]$ greater than about 100 μM, only the induced state exists.

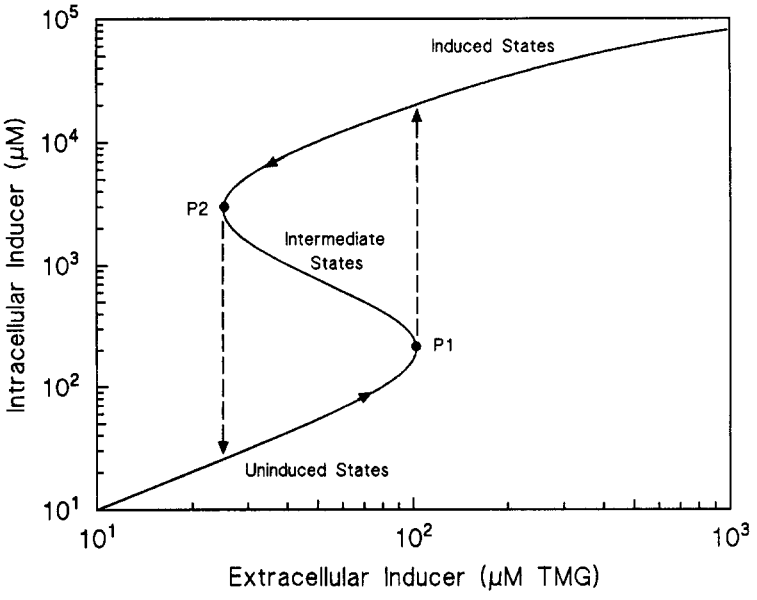

Fig. 8. Hysteresis curve depicting the dependence that the transcriptional state of the cell, as defined by its intercellular concentration of inducer, has on the cell's previous history.

dependence exhibits a hysteresis that may be explained by observing the behavior of a cell as it traverses the closed path shown in Fig. 8 in the direction of the arrows.

Figure 8 is consistent with other reported observations. The induction threshold or 'jump' that occurs at approximately 100 μM TMG is consistent with the experimental protocol of Novick and Wiener (1957) who used 250–500 μM TMG to obtain fully induced cultures. Also described is the ability of cells to concentrate inducer. Rickenberg and coworkers (1956) and Kepes (1960) found that induced cells could concentrate inducer to levels approximately 100 times that of the extracellular medium. This concentration factor is described over a large range of $[I_{EX}]$. The agreement between the threshold $[I_{EX}]$ at P2 is exact (Novick and Wiener, 1957) since it represents a fit (Fig. 6, curve 2).

3.7. *Heterogeneity associated with the induction of the operon*

Physiological heterogeneity in a culture can be generated by stochastic processes affecting the distribution of permease throughout the cell population. This may be explained with reference to Fig. 9 where the steady-state value of the number of permease molecules per cell has been determined at different $[I_{EX}]$ using eqs (35) and (36) assuming a cell volume of 1×10^{-15} l. The branches of this curve correspond identically to those shown in Fig. 8. Since the average number of permease molecules per cell on the uninduced branch is estimated to be on the order of 10, the partitioning of permease molecules upon cell division might be expected to add significant variability to the culture population particularly under conditions of intermediate $[I_{EX}]$. For example, if an uninduced mother cell were to unequally partition its permease molecules (approximately 20 assuming the cell has doubled in volume) such that one daughter cell received them all, then the smaller volume of the daughter cell would result in a permease concentration of approximately twice that of the mother cell. If such an increase in the absolute number of permease molecules allows the daughter cell to overcome the 'permease barrier' (Fig. 9) by placing it above the intermediate solution branch, it will eventually acquire the induced state. The fact that the entire cell population never acquires the induced state, even after sufficiently large number of generations, originates from the growth rate advantage that uninduced cells have over induced cells (Novick and Weiner, 1957).

Figure 9 is consistent with a number of experimental observations. Novick and Weiner (1957, 1959) originally proposed that a threshold number of permease molecules on the order of 2–3 per cell were needed before the cell could acquire the induced state. It has also been estimated that the number of functional permease until per cell at the fully induced state is about 200 (Cohn and Horibata, 1959). Figure 9 indicates that the number of permease units pe r cell at P1 and P2 correspond to approximately 5 and 500, respectively. Since a degree of variation exists along all branches of the curve, these results are reasonable. Figure 9 also predicts that as $[I_{EX}]$ is increased, the chance that an uninduced cell will acquire the induced state also increases due to a decrease in the 'permease barrier' as P1 is approached. This prediction agrees with the findings of Novick and Weiner (1957).

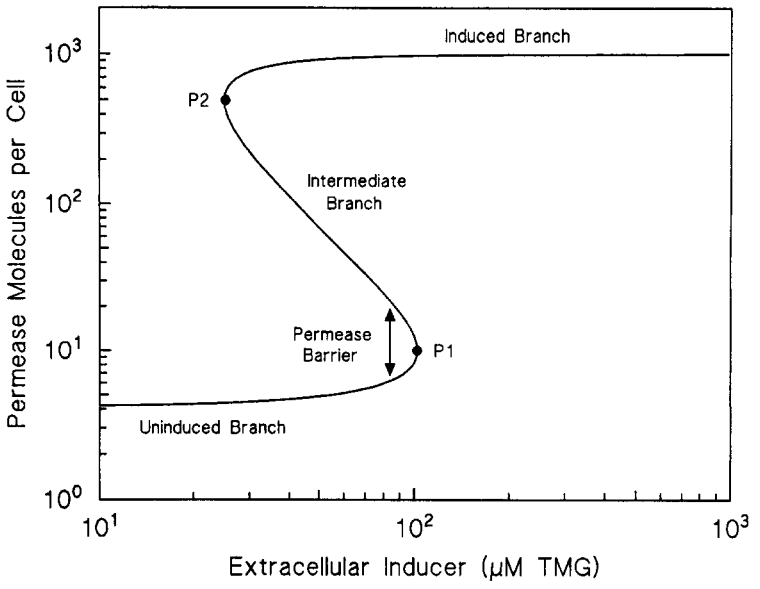

Fig. 9. Hysteresis curve depicting the number of permease moleculars per cell at different $[I_{EX}]$. Since the number of permease molecules per cell can be expected to roughly double during the lifetime of a given cell, this figure is meant to represent the number of permease molecules contained by the average newborn cell assuming a cell volume of 1×10^{-15} l.

4. DISCUSSION

Through the application of fundamental physical principles, information reported on two classical genetic systems has been used to construct an unambiguous and perhaps different picture of how physico-chemical processes interact in order to initiate adaptive cellular behavior. Within this framework, the option to adopt an alternate physiological state relied on the existence of alternate or multiple *stable* states of the representative balance equations. In cases where unique solutions existed, adaptation was not possible. However, the actual decision to initiate a transition has found to rely on intracellular rate imbalances, created by external perturbations that caused a departure from the existing cellular state. The fact that small perturbations in certain parameters could effect the transition indicate that threshold mechanisms are involved. Therefore, this analysis allows us to view adaptation and adaptive gene expression as all-or-none phenomena.

This study has also made it possible to investigate how stochastic and deterministic processes generate physiological heterogeneity. Deterministic processes were found to play central roles in defining the developmental options via the interactions of the molecular genetic mechanisms. As alluded to above, these options were manifested through the existence of nonunique solutions of the governing material balances. Yet, under the appropriate typically suboptimal induction conditions, random processes can play an important role in deciding which cells among the population "adapt". With phage, it was found that slight variations in intracellular repressor or activated RecA could lead phage to very different developmental fates. The partitioning of *lac* permease during cell division would also be expected to be governed by chance. Given the relative simplicity of these systems, it is possible to conclude that random and deterministic mechanisms play important roles in generating heterogeneity in higher organisms.

Despite the apparent differences between the *lac* and the phage systems, this analysis has provided the means of identifying and appreciating the conserved biological structures involved in generating physiological heterogeneity. So long as the adaptive process is regulated by a positive feedback loop and a nonlinear generation term, of the cooperative type, the potential for multiple steady states exists. With phage, positive feedback results from the fact that repressor activates its own expression. With the *lac* operon, positive feedback results from the fact that permease indirectly activates its own rate of expression via inducer. The second crucial structural element involved is the nonlinear generation rate which in both cases originate from the need for *two* molecules of either CI dimer or *lac* inducer to initiate transcription. This led to generation rate curves that exhibited points of inflection (i.e. S-shaped curves) which when combined with the appropriate removal rates, predicted the existence of multiple stable steady states. Had linear forms of the generation rate expressions been adopted by requiring that only one molecule of CI or *lac* inducer be sufficient to initiate transcription, a much different dynamical system would have resulted. In such cases only one stable steady state would have been predicted theoretically so that the simple models

presented would have not been capable of explaining how nonunique cell types can stably coexist within the same environment.

The ability of these simple models to provide explanations for a variety of complex biological behavior and to further explore the cellular processes associated with adaptation, is significant in several respects. First, it demonstrates that complex biological behavior can originate from simple mechanisms, all of which can be found in biological systems currently being studied. Second, it demonstrates that the use of complicated biological models does not necessarily increase one's ability to accurately capture the salient physics. Finally, this work justifies the calls for quantativity biological data (Maddox, 1992) by providing a framework in which to seek and to analyze quantitative data. If an eventual goal in biology is to explain complex biological behavior, qualitative or descriptive data alone will not suffice in the long run.

Acknowledgement—Financial support from the National Science Foundation, Grant No. EET-8711725 and BCS-9311509, is gratefully acknowledged.

NOTATION

$[CI]$	concentration of CI monomer
$[(CI)_2]$	concentration of CI dimer
$[I]$	concentration of *lac* inducer
$[I_{EX}]$	concentration of extracellular *lac* inducer
$[I_2R]$	concentration of *lac* repressor–inducer complex
K_a	equilibrium constant associated with the CI dimerization reaction
K_A	apparent equilibrium constant associated with the CI dimerization reaction
k_f	forward rate constant for the CI dimerization reaction
k_r	reverse rate constant for the CI dimerization reaction
k_1	first-order rate constant for the CI or the *lac* permease generation reaction
k_2	first-order rate constant representing the dilution CI or *lac* permease due to cell growth
k_3	rate constant representing the degradation of CI dimer
K_1	equilibrium constant associated with the binding of CI dimer to the unoccupied O_R operator or the *lac* repressor–inducer equilibrium constant
K_2	equilibrium constant associated with the binding of CI dimer to singly occupied O_R complex or the *lac* repressor–operator equilibrium constant
K_3	equilibrium constant associated with the binding of CI dimer to the doubly occupied O_R complex
$[O]$	concentration of free O_R or *lac* operator
$[O_T]$	concentration of total O_R or *lac* operator
$[O(CI)_2]$	concentration of singly occupied O_R
$[O(CI)_2(CI)_2]$	concentration of doubly occupied O_R
$[O(CI)_2(CI)_2]$	concentration of triply occupied O_R
R_{ACTIVE}	rate of active transport of *lac* inducer *via* permease
$R_{FACILITATED}$	rate of facilitated transport of *lac* inducer
R_{GEN}	CI or *lac* permease generation rate
$[R]$	concentration of free *lac* repressor
$[RO]$	concentration of *lac* repressor–operator complex
$[R_T]$	total concentration of *lac* repressor
t	time
V_c	cell volume
$[Y]$	concentration of *lac* permease

Greek letters

α	permease turnover number
β	permease saturation constant
δ	*lac*-inducer-facilitated transport coefficient
τ	cell-doubling time

REFERENCES

Ackers, G. K., Johnson, A. D. and Shea, M. A., 1982, Quantitative model for the regulation by λ phage repressor. *Proc. Natl. Acad. Sci. U.S.A.* **79**, 1129–1133.

Bailey, J. E. and Ollis, D. F., 1986, *Biochemical Engineering Fundamentals*, pp. 429–432. McGraw Hill, New York.

Bailone, A., Levine, A. and Devoret, R., 1979, Inactivation of prophage λ repressor *in vivo*. *J. Molec. Biol.* **131**, 553–572.

Barkley, M. D. and Bourgeois, S., 1980, in *The Operon* (Edited by J. H. Miller, and S. W. Reznikoff), pp. 177–220. CSH Laboratory, USA.

Benzer, S., 1953, Induced synthesis of enzymes in bacteria analyzed at the cellular level. *Biochim. Biophys. Acta* **11**, 383–395.

Boezi, J. A. and Cowie, D. B., 1961, Kinetic studies of β-galactosidase induction. *Biophys. J.* **1**, 639–647.

Bourgeois, S. and Monod, J., 1970, *In vitro* studies of the *lac* operon regulatory system, in *Control Proceses in Multicellular Organisms* (Edited by G. E. W. Wolstenholme and J. Knight), pp. 3–27. J&A Churchill, London.

Chadwick, P., Pirrotta, V., Steingerg, R., Hpokins, N. and Ptashne, M., 1970, The λ and 434 phage repressors. *Cold Spring Harbor Symp. quant. Biol.* **35**, 283–294.

Chung, J. D., 1994, Ph.D. Dissertation, Massachusetts Institute of Technology.

Chung, J. D., Stephanopoulos, G. S., Ireton, K. and Grossman, A. D., 1994, Gene expression in single cells of *Bacillus subtilis*: Evidence that a threshold mechanism controls the initiation of sporulation. *J. Bact.* **176**, 1977–1984.

Cohn, M. and Horibata, K., 1959, Analysis of the differentation and of the heterogeneity within a population of *Escherichia coli* undergoing induced β-galactosidase synthesis. *J. Bact.* **78**, 613–623.

Cohen, G. H. and Monod, J., 1957, Bacterial permeases. *Bact. Rev.* **21**, 169–194.

Darnell, J., Lodish, H. and Baltimore, D., 1990, *Molecular Cel Biology*, pp. 245–246. Scientific American Books, New York.

Herzenberg, L. A., 1959, Studies on the induction of β-galactosidase in a cryptic strain of *Escherichia coli*. *Biochem. Biophys. Acta* **31**, 525–538.

Horvitz, H. R. and Herskowitz, I., 1992, Mechanisms of asymmetric cell division: two Bs or not two Bs, that is the question. *Cell* **68**, 237–255.

Jacob, F. and Monod, J., 1961, Genetic regulatory mechanisms in the synthesis of proteins *J. Molec. Biol.* **3**, 318–356.

Johnson, A. D., Poteete, A. R., Lauer, G., Sauer, R. T., Ackers, G. K. and Ptashne, M., 1981, λ repressor and cro-components of an efficient molecular switch. *Nature, Lond.* **294**, 217–223.

Kepes, A., 1960, Etudes cinetiques sur la galactoside-permease D'*Escherichia coli. Biochim. Biophys. Acta* **40**, 70–84.

Laffend, L. and Shuler, M. L., 1994, Structured model of genetic control via the *lac* promoter in *Escherichia coli. Biotechnol. Bioengng* **43**, 399–410.

Maddox, J., 1992, Is molecular biology yet a science? *Nature, Lond.* **355**, 201.

Maloney, P. C. and Rotman, B., 1973, Distribution of suboptimally induced β-D-galactosidase in *Escherichia coli. J. Molec. Biol.* **73**, 77–91.

Novick, A. and Weiner, M., 1957, Enzyme induction as an all-or-none phenomenon. *Proc. Natl. Acad. Sci. U.S.A.* **43**, 553–566.

Novick, A. and Weiner, M., 1959, The kinetics of β-galactosidase induction, in *A Symposium on Molecular Biology* (Edited by R. E. Zirkle), pp. 78–90. Uni. Chicago Press, Chicago.

Pirotta, V., Chadwick, P. and Ptashne, M., 1970, Active from of two coliphage repressors. *Nature, Lond.* **227**, 41–44.

Ptashne, M., 1987, *A Genetic Switch: Gene Control and Phage Lambda.* Cell Press, Cambridge, MA and Blackwell Science, Palo Alto, CA.

Rickenberg, H. V., Cohen, G. N., Buttin, G. and Monod, J., 1956, La galactoside-permease D'*Escherichia coli. Ann. Inst. Pasteur, Paris* **91**, 829–857.

Yagil, G. and Yagil, E., 1971, On the relationship between effector concentration and the rate of induced enzyme synthesis. *Biophys. J.* **11**, 11–27.